Nanoveneers: An Electrochemical Approach to Synthesizing Conductive Layered Nanostructures

Xiaojun Xian, Liying Jiao, Teng Xue, Zhongyun Wu, and Zhongfan Liu*

Centre for Nanochemistry, Beijing National Laboratory for Molecular Sciences, State Key Laboratory for Structural Chemistry of Unstable and Stable Species, College of Chemistry and Molecular Engineering, Peking University, Beijing 100871, People's Republic of China

ABSTRACT We report herein a facile electrochemical approach to synthesizing various layered composite films of nanomaterials and conducting polymers, called *nanoveneers*. Layered structures of polypyrrole film with single-walled carbon nanotubes (SWNTs), graphene, and Au nanoparticles have been obtained by electropolymerization of pyrrole molecules on a heavily doped silicon wafer preloaded with target conductive nanomaterials. A free-standing, transparent, and highly conductive composite film was achieved after peeling off from a silicon wafer. Different from traditional homogeneous composite materials, such kinds of nanoveneers combined to the best extent the structural continuity and processability of conducting polymers with the high conductivity and functionality of discontinuous SWNTs, graphene, and other nanomaterials. The layered electrochemical deposition provides a great freedom for constructing various nanostructures with well-controlled geometry and thus physicochemical properties, as demonstrated by SWNT/polypyrrole nanoveneers. These nanoveneers are particularly attractive in areas of chemical sensors, labels, transparent electronics, and optoelectronics.

KEYWORDS: nanoveneer · electropolymerization · SWNTs · graphene · nanoparticles

The emergence of various conductive nanomaterials such as zero-dimensional (0D) fullerenes, quantum dots and nanoparticles, 1D carbon nanotubes and nanowires, and 2D graphene over the last two decades provides a great driving force for developing micro-, nano-, and opto-electronic devices.[1−6] The hybridization of these nanomaterials with conducting polymers as highly functional composite films and structures has enriched the space of exploration especially on chemical and bio-sensors,[7−9] solar cells,[10−12] high-performance electrochemical electrodes,[13,14] supercapacitors,[15] and high-strength artificial muscles.[16] The conventional approaches to preparing nanomaterial/polymer composite films include solution phase mixing followed by solvent evaporation,[17,18] mixing nanomaterials with a monomer precursor followed by polymerization,[19−21] and directly casting a polymer into the nanomaterial layer,[22−24] which in principle leads to a homogeneous composite film with the discontinuous nanomaterials being uniformly dispersed into the continuous polymer matrix. One of the intrinsic shortcomings of such homogeneous hybridization techniques is the damping, or, say, dilution effect, of the excellent functionalities of nanomaterial components by the polymer phase. On the other hand, spontaneous aggregation of nanomaterials followed by segregation from the polymer matrix is also a troublesome issue, originating from their high surface energy and different chemical nature from polymer backbones. We report herein an alternative hybridization methodology of combining polymers with functional nanomaterials to overcome these intrinsic problems with a facile electrochemical layered deposition approach. Instead of homogeneous hybridization of components, the discontinuous phase, such as SWNTs and nanoparticles, is firmly adhered to the continuous polymer phase, forming a layered structure. Such kinds of layered nanomaterials/polymer films can be called *nanoveneers*. We will demonstrate the electrochemical synthesis of various nanoveneers and their structural engineering for modulating electrical and optical properties.

Figure 1 shows the schematic illustration of electrochemical methodology to synthesize conductive nanoveneers and the derived film structures using SWNT/polypyrrole nanoveneer as an example. The pristine SWNT array is first loaded onto a heavily doped silicon wafer, which is then serving as the working electrode to perform electropolymerization of pyrrole molecules in an electrochemical cell (see Figure 1a). The structural discontinuity of SWNTs allows for easy penetration of pyrrole species and

* Address correspondence to zfliu@pku.edu.cn.

Received for review February 11, 2011 and accepted April 7, 2011.

Published online April 07, 2011
10.1021/nn200566q

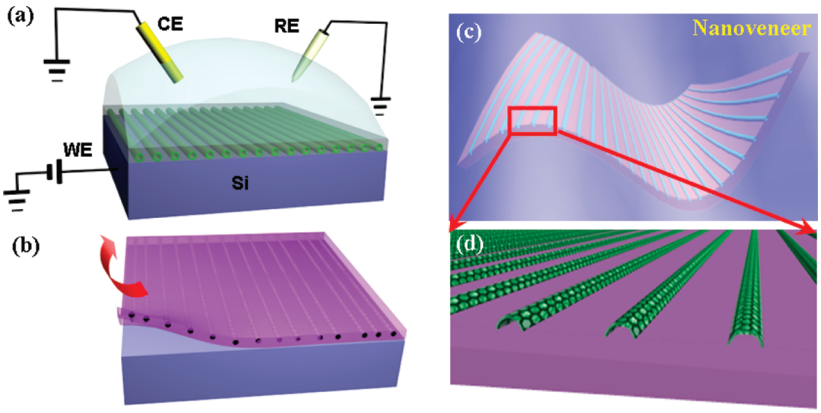

Figure 1. Schematic illustration of electrochemical synthesis of conductive nanoveneers. (a) Electrochemical arrangement using a working electrode of heavily doped silicon wafer on which the target conductive nanomaterials are preloaded. The counter and reference electrodes were Pt wire and SCE, respectively, and the electrolyte was 25 mmol/L pyrrole/100 mmol/L sodium dodecyl sulfate (SDS). (b) Peeling off the nanoveneer from silicon wafer electrode after electrochemical deposition of conducting polymer film. (c, d) Structural illustration of SWNT/polypyrrole nanoveneer with SWNT array being half-embedded into polypyrrole film.

their ubiquitous polymerization on a silicon surface. The high electrical conductivity of SWNTs may also provide additional sites of polymerization. These effects ensure the formation of layered composite structures and the firm adherence of SWNTs on the surface of a polypyrrole film (see Figure 1c and d). Because of the weak van der Waals interactions, such kinds of composite films can be easily peeled off from a silicon electrode, forming a free-standing and transparent conducting film (see Figure 1b). Obviously, this on-site electropolymerization technique can be applied to the synthesis of conducting polymer nanoveneers with arbitrary conductive nanomaterials such as metallic and semiconducting nanowires/nanotubes, nanoparticles, and graphene. In principle, ultrathin multilayer nanoveneers are also available *via* a layered electrochemical deposition.

RESULTS AND DISCUSSION

Figure 2a–d demonstrates various conductive nanoveneers of polypyrrole with a SWNT crossbar array, random SWNT film, SWNT parallel array, and gold nanoparticles synthesized by our electropolymerization approach. The electropolymerization was conducted on heavily doped silicon wafers preloaded with target nanomaterials in 25 mmol/L pyrrole/100 mmol/L sodium dodecyl sulfate aqueous solution at 0.8 V (see Supporting Information (SI) for the experimental details). Free-standing nanoveneers were obtained by peeling off from silicon substrates simply using Scotch tape after overnight immersion in acetone. As clearly seen from the scanning electron microscope (SEM) images in Figure 2a–d, all the target nanomaterials are embedded on the surface of the polypyrrole film, forming layered veneer structures. In the case of SWNT/polypyrrole nanoveneers, Raman spectroscopy shows the characteristic radial breathing mode (RBM) and G bands of SWNTs (see SI, Figure S1), further confirming that the SWNT film was located at the polypyrrole surface as expected. It is believed that the unique layered structures of such composite films are attributed to the peculiar electrosynthesis process. Because of the high porosity of a discontinuous phase such as SWNTs and gold nanoparticles, pyrrole species can easily diffuse to the close vicinity of the silicon electrode surface and get electropolymerized. This results in the formation of a continuous polypyrrole film enwrapping the discontinuous nanomaterials. The excellent electrical conductivity of the employed nanomaterials could remarkably reduce the potential drop at the surface normal direction. As a consequence, at least some of the conductive nanomaterials could also serve as the working electrode for electropolymerization of pyrrole molecules, which undoubtedly facilitates the firm embedment of discontinuous nanomaterials onto the polymer matrix. On the other hand, the van der Waals contact between the silicon electrode surface and nanomaterials would inhibit a perfect enwrapping of nanomaterials by the polypyrrole film, leading to the easy detachment of such nanoveneers from deposition substrates. As shown in Figure 2a–c, the original morphology of the SWNT film can be perfectly preserved on the nanoveneer surface after peeling off from the deposition substrate. Figure 2e exhibits a three-layer nanoveneer of graphene/polypyrrole/graphene made by repeating the transfer-printing[25] and electropolymerization processes. In this case, both sides are terminated by highly conductive graphene films. Hence such a sandwiched nanoveneer can function as a nanocapacitor assuming that the polypyrrole layer is undoped.

Our electrochemical approach provides a convenient way to engineer the nanoveneer structures. Simply by controlling the deposition time, we can regulate the thickness of the polypyrrole layer in the nanoveneers. For instance, the thickness of random SWNT film/

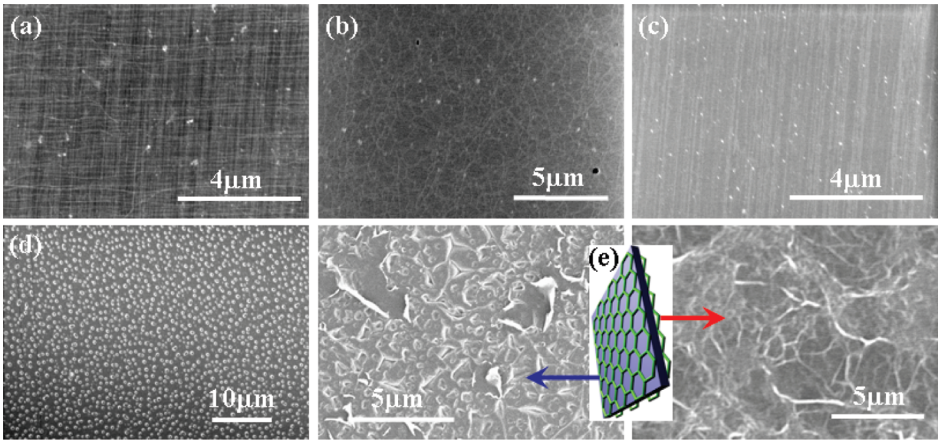

Figure 2. SEM images of various conductive nanoveneers. (a) SWNT crossbar/polypyrrole (thickness: 95 nm). (b) Random SWNT film/polypyrrole (thickness: 85 nm). (c) SWNT parallel array/polypyrrole (thickness: 95 nm). (d) Au nanoparticles film/polypyrrole (Au nanoparticle diameter: 50 nm; thickness: 120 nm). (e) Graphene/polypyrrole/graphene (thickness: 139 nm). For the bilayer nanoveneer preparation, before polypyrrole deposition, SWNTs were loaded on a heavily doped silicon wafer *via* transfer-printing, while Au nanoparticles were loaded *via* spin-coating. As for the graphene/polypyrrole/graphene nanoveneer, the first graphene layer was transferred on the Si wafer followed by polypyrrole deposition, and the second graphene layer was transferred onto the other side of the polypyrrole layer by transfer-printing. The electropolymerization was conducted in 25 mmol/L pyrrole/100 mmol/L SDS solution at 0.8 V *vs* SCE (see SI).

polypyrrole nanoveneer was nearly proportional to the deposition time at a constant potential of 0.8 V *vs* SCE (see SI, Figure S2). This enables the optical transmittance modulation of nanoveneers as seen in Figure 3a. The random SWNT film/polypyrrole nanoveneer with a thickness of 90 nm was nearly transparent in the visible region. At 550 nm, the transmittance is linearly increased with the decrease of film thickness. The upper inset of Figure 3a shows a photograph of this nanoveneer laid on a paper with our university logo, demonstrating its excellent optical transparency. As shown in the lower inset of Figure 3a, the transparency is nearly 70% at 250−850 nm. In fact, the polypyrrole layer of this nanoveneer dominated the optical transmittance because the original SWNT film had a transparency of over 95% at the same wavelength region (see SI, Figure S3). Of great importance is the electrical performance of such kinds of nanoveneers. Figure 3b compares the distinct electrical properties of pure polypyrrole film and random SWNT network/polypyrrole nanoveneer. Together with the increase of film thickness, both of them show an exponential decrease in sheet resistance, consistent with the previous results.[26] However, although the SWNT film is only a few nanometers thick, the nanoveneer exhibits a drastic increase of electrical conductance. This is certainly attributed to the unique layered structure of the SWNTs/polypyrrole nanoveneer, in which the highly conductive SWNTs are embedded on the film surface rather than a homogeneous dispersion into the polymer matrix. The increase of electrical conductance becomes more and more remarkable in response to a decrease of film thickness. For instance, the sheet resistance of a random SWNT network/polypyrrole nanoveneer is only one-fourth of the pure polypyrrole film at a thickness of *ca*. 100 nm. It is well known that conducting polymers such as polypyrrole are not stable in air and their electrical conductivity gradually decreases due to oxidative degradation.[27] The conductivity of conducting polymers is also very sensitive to the environment, especially to a basic environment because of the dedoping effect.[28] These drawbacks limited their potential applications in electronics. For a nanoveneer with its electrical characteristics being dominated by the chemically stable SWNTs, the electrical stability can be greatly improved. We compared the sheet resistance changes of random SWNT network/polypyrrole nanoveneer and pure polypyrrole film after treatment with ammonia solution. In the case of the pure polypyrrole film, the sheet resistance increased by *ca*. 5 orders of magnitude. In contrast, the SWNT/polypyrrole nanoveneer showed an increase of only 49% (see SI, Figure S4), exhibiting its stability to the surrounding conditions.

The physicochemical properties of nanoveneers can be further modulated by using different nanomaterials and/or by designing the morphology of the employed nanomaterials. Again the SWNT/polypyrrole system was taken as an example. We synthesized two different types of SWNT/polypyrrole nanoveneers and carried out two-terminal *I*−*V* measurements as shown in Figure 4a,b. With an aligned SWNT array embedded on the polypyrrole film, it shows a strong anisotropy in electrical conductance (Figure 4a). The conductance along the SWNT direction was 6.5-fold higher than the perpendicular direction. On the other hand, with a SWNT crossbar/polypyrrole nanoveneer, the electrical conductance did not show substantial differences along different directions (Figure 4b). This suggests that one can perform a delicate structural engineering to tune the physical properties of nanoveneers using our electrosynthesis approach.

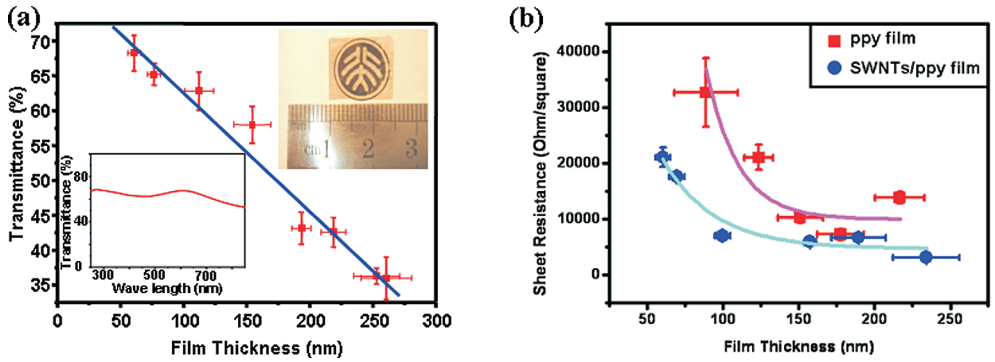

Figure 3. (a) Transmittance-film thickness dependence of a random SWNT network/polypyrrole nanoveneer at 550 nm. Upper inset is the photograph of such a nanoveneer laid on our university logo, demonstrating its optical transparency. Lower inset is the transmittance spectrum of the layered composite film with a thickness of 90 nm. (b) Sheet resistance–film thickness dependences of pure polypyrrole film (red) and random SWNT network/polypyrrole nanoveneer (blue).

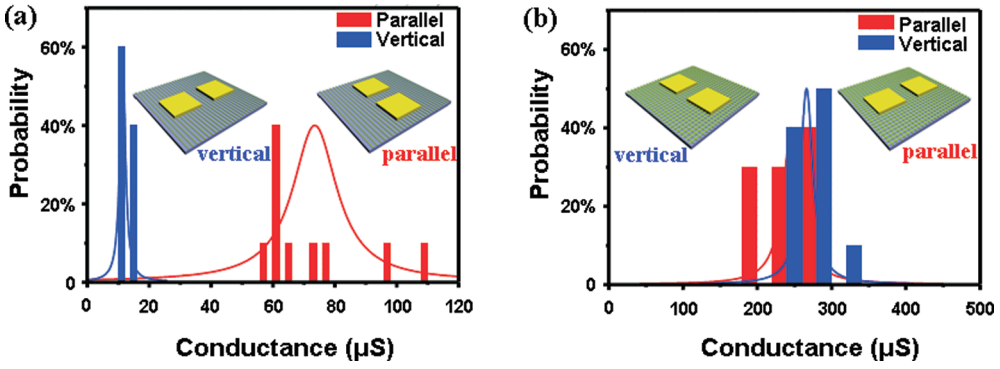

Figure 4. Conductance statistics along parallel and vertical directions of (a) parallel SWNT array/polypyrrole and (b) SWNT crossbar/polypyrrole nanoveneers. The film thicknesses in both cases are approximately 95 nm. SWNTs array was synthesized by the CVD method and then transferred onto a silicon wafer for polypyrrole deposition. The average density was about 20 tubes/μm, and the length was about hundreds of micrometers. SWNT crossbar was obtained by transferring the SWNT array twice onto the silicon wafer along the perpendicular direction, and then polypyrrole deposition was carried out.

The unique layered structure and designable interface of our conductive nanoveneers offer great freedom for developing transparent electronic and optoelectronic devices, sensors, labels, and highly functionalized films. We demonstrate here a chemical sensor based on our SWNT/polypyrrole nanoveneer. The basic requirement for a typical chemical sensor is to convert a molecular binding event into a measurable electrical signal. As for a field-effect transistor (FET)-based chemical sensor, the molecular binding takes place at the surface/interface of the channel materials.[29] Therefore, the designability of this surface/interface is of particular importance for creating a purpose-specific chemical sensor. Both SWNTs and polypyrrole have been reported to show electrical response to ammonia species.[30,31] The nanometer-scale ultrathin SWNT phase and its designability allow for combination of the sensing performances of SWNTs and polypyrrole as the conducting channels. We fabricated an ammonia gas sensor using our SWNT/polypyrrole nanoveneers as schematically shown in Figure 5a, in which vacuum-evaporated gold pads were employed as the drain and source electrodes. Figure 5b,c exhibits a photograph of the whole sensor device and the optical microscope image of the channel area, respectively. The normalized current response-time characteristic of this ammonia gas sensor is shown in Figure 5d (red curve). In response to ammonia gas exposure, the current signal of the nanoveneer sensor exhibits a sharp decrease with a level of up to 8%. As reported previously, both SWNTs and polypyrrole show p-type transport behavior in the composite.[7] Adsorption of ammonia species to SWNTs and polypyrrole both reduce the hole density in the conduction channel and hence increase the resistance. As seen from Figure 5d (red curve), the nanoveneer sensor exhibited an excellent reproducibility with repeating ammonia gas and N_2 gas injection. Upon nitrogen gas purging, the current response was mostly recovered. As a control experiment, we also fabricated pure SWNTs and polypyrrole sensors for comparison, as shown in Figure 5d (blue and green curves, respectively). It is obvious that the sensing performance of the SWNT sensor degrades very rapidly. As for the polypyrrole sensor, it took a very long time for recovery of the current signal upon N_2 purging. We calculated the detection limits for SWNT/polypyrrole, SWNT, and polypyrrole sensors, which were 120, 105, and 41 ppm, respectively. The SWNT/

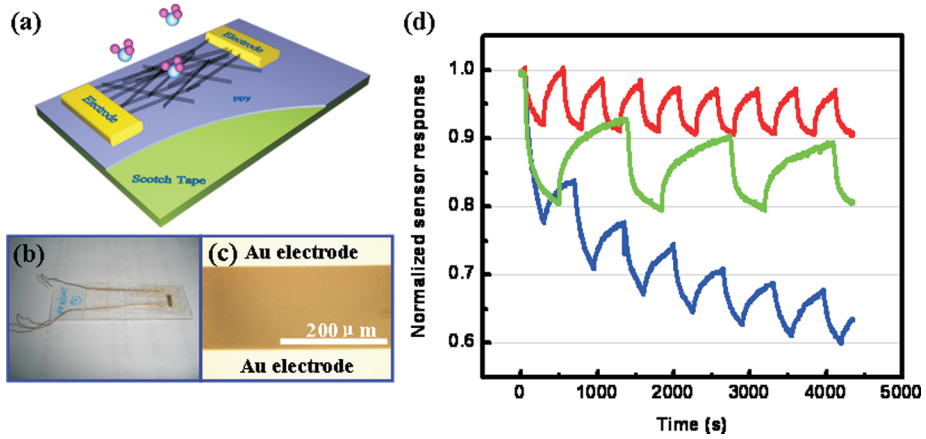

Figure 5. Ammonia sensor using random SWNT network/polypyrrole nanoveneer. (a and b) Schematic illustration and photograph of the sensor structure. (c) Optical microscope image of the sensor channel area. (d) Normalized current responses of SWNT/polypyrrole nanoveneer sensor (red, thickness: 185 nm), pure SWNT sensor (blue), and pure polypyrrole sensor (green, thickness: 170 nm) to 960 ppm ammonia gas (channel length: 200 μm; channel width: 1 mm; bias: 0.001 V).

polypyrrole sensor has a similar detection limit to the SWNT sensor, but the performance is far more stable and reproducible. Although the polypyrrole sensor shows a better detection limit than the SWNT/polypyrrole sensor, the response is very slow. Furthermore, the polypyrrole sensor is not stable and sensitive to the environmental conditions (refer to Figure S4). Therefore it is obvious that our SWNT/polypyrrole sensor has the best overall sensor performance. The excellent performance of the nanoveneer sensor definitely originates from its unique surface/interface structure. Because of the distinct chemical natures, desorption of ammonia molecules would be easier from the SWNT surface than from the polypyrrole matrix. The excellent thermal conductivity of SWNTs would help to rapidly spread the current joule heat over the whole sensor channel, which also accelerates the desorption of ammonia molecules. These effects are believed to be responsible for the fast recovery of nanoveneer sensors. Finally, it should be mentioned that such nanoveneer sensors are transparent and can be easily adhered to any location for various sensing purposes.

Moreover, the unique structure of the SWNT/polypyrrole nanoveneer also makes it possible to fabricate a SWNT thin film transistor simply by changing the polypyrrole layer into an insulating state *via* dedoping. As shown in Figures S5,6, such kinds of SWNT FETs exhibit similar performance, as previously reported.[32]

CONCLUSION

In conclusion, we have developed a facile electropolymerization technique for synthesizing unique nanoveneers of nanomaterials and conducting polymers. Different from the homogeneous dispersion of conventional composite films, the electrically conductive nanomaterials are firmly attached to the polymer matrix, forming a layered film and structures. Such kinds of nanoveneers are conductive, with excellent optical transparency, and well combine the functions and advantages of the components. Of particular importance is its high freedom of structural designability. With a delicate design and control of nanomaterial type and morphology, surface/interface structure, thickness, and doping and undoping of polymer matrix, we can easily tune the physicochemical properties of these nanoveneers. In principle, any type of conductive nanomaterials can be employed as the functional components of these nanoveneers, including metallic and semiconducting 0D fullerenes and nanoparticles, 1D nanowires and nanotubes, and 2D graphenes. We believe that our nanoveneers would provide a great space and freedom for fabricating various electronic and optoelectronic devices, sensors, labels, and high-performance thin films.

METHODS

Synthesis of SWNTs, Graphene, and Au Nanoparticles. SWNTs were synthesized by the chemical vapor deposition (CVD) method. The aligned SWNT array was grown on sapphire according to the method given by Zhang *et al.*[33] Sapphire substrates with a single-polished a-plane (1120) were cleaned with acetone, hydrochloric acid, and ultrapure water, followed by annealing at 1100 °C in air for 2 h. $Fe(OH)_3$ colloids were spin-coated on annealed sapphire at 2000 rpm. The aligned carbon nanotube array was grown at 850 °C for 5 min by bubbling ethanol containing 3 wt % deionized water. The average density was about 20 tubes/μm, and the length was about hundreds of micrometers. A high-density random network of SWNTs was grown on a SiO_2/Si wafer following the approach of Choi *et al.*[34] Silicon wafers with a 800 nm SiO_2 layer were treated in piranha solution at 90 °C for 15 min and then immersed in a freshly

mixed aqueous solution of $FeCl_3$ and hydroxylamine to form catalyst particles on the surface. After that, the substrates were calcined at 800 °C for 5 min in air. CVD growth of such SWNTs was carried out at 970 °C for 30 min by using CH_4 as the carbon source.

Graphene oxide was dispersed into the water after dialysis. It was then centrifuged at 6700 rpm for 10 min to remove the undissolved graphene oxide. Then the solution was diluted by solvent that was mixed with methanol and water (v/v = 2:1), and the coating solution with a concentration of 0.5 mg/mL was obtained. Next, 30 μL of coating solution was dropped on the silicon wafer and then dried under vacuum at 75 °C. The graphene oxide thin film was reduced in a tube furnace at 1100 °C for 70 min under 300 sccm argon and 100 sccm hydrogen flow. Finally we obtained the reduced graphene film with a thickness of about 7 nm.

Au nanoparticles with a diameter of 50 nm were synthesized by the method given by Niu *et al.*[35] Then the Au nanoparticle solution was spin-coated onto a heavily doped silicon wafer for polypyrrole deposition.

The SWNT crossbar was obtained by transfer-printing a SWNT array twice onto a heavily doped silicon wafer along the perpendicular directions.[25]

Loading Nanomaterials onto Heavily Doped Silicon Wafer. SWNTs and graphene were transferred from their original substrates onto a heavily doped silicon wafer by using the PMMA-mediated nanotransfer-printing technique we developed recently.[25] Briefly, PMMA was spin-coated onto the substrates growing SWNTs or graphene to form a thin layer and then baked at 170 °C for 30 min. Then the substrate was immersed in KOH solution (10 g in 50 mL of H_2O) and heated to boiling. After peeling off from the original substrate, the PMMA film was rinsed with ultrapure water and then laid onto the heavily doped silicon wafer, which had been pretreated with HF solution to remove the oxide layer. The wafer with the PMMA layer was carefully subjected to a N_2 gas stream until it was dry and tightly adhered to the wafer surface. Then the wafer was immersed in acetone to dissolve the PMMA layer thoroughly, leaving the target nanomaterials on the silicon wafer as the working electrode for electropolymerization.

Electropolymerization and Peeling off of Free-Standing Nanoveneers. The potentiostatic method was used for electropolymerization of pyrrole using a CHI-710 electrochemical workstation. A platinum wire was used as a counter electrode, and SCE was used as a reference electrode. The electrolyte solution consisted of 25 mmol/L pyrrole and 0.1 mol/L SDS. A heavily doped silicon wafer preloaded with target nanomaterials was used as a working electrode to electropolymerize pyrrole molecules at a potential of 0.8 V to form a thin polypyrrole film on the wafer surface. Then the wafer with the composite film was dipped into acetone overnight to weaken the adherence between the silicon substrate and the composite film. After that, the substrate was dried with nitrogen gas. The composite film was then mechanically peeled off using Scotch tape from the wafer surface.

Characterization. The composite nanoveneers were characterized by a Hitachi 4800 scanning electron microscope (SEM) typically at 1 kV. The AFM characterization was carried out on a Nanoscope III SPM (Veeco) in tapping mode. A Renishaw micro-Raman system (1 μm spot size, He−Ne laser) with 633 nm (1.96 eV) laser excitation was used to obtain the resonant Raman spectra of SWNTs. Sheet resistance measurements were carried out on a probe station using a Keithley 4200 semiconductor characterization system in the four-probe configuration. Before electrical measurements, a *ca.* 50 nm Au thin film was deposited *via* thermal evaporation on top of the as-prepared composite film through a shadow mask to form a well-aligned electrode array. The area of each electrode pad was 70 × 70 μm^2, and the channel length between two neighboring electrode pads was 30 μm. The electrical measurement was done by using microprobes directly contacting the Au electrode pads.

Sensor Fabrication and Test. The random SWNT film/polypyrrole nanoveneer was prepared according to the method mentioned above. A Cu wire with a diameter of 200 μm was placed at the center of the nanoveneer to serve as a mask. The 80 nm Au film was deposited onto the nanoveneer to form source and drain electrodes by thermal evaporation. This device was located in the chamber of a homemade sensor test equipment for sensing performance measurement. A Keithley 4200 semiconductor characterization system was used to apply a bias of 0.001 V between the source and drain electrodes during the test. The gas injection was switched between 960 ppm ammonia gas and nitrogen during the test.

Fabricating SWNT Thin Film Transistor from SWNT/Polypyrrole Nanoveneers. The schematic illustration of the experimental procedure for fabricating a SWNT thin film transistor from a SWNT/polypyrrole composite film is shown in Figure S5. Briefly, after deposition of polypyrrole onto the SWNT film, an 80 nm Au layer was deposited on top of the polypyrrole, which could serve as the gate electrode. Then the SWNT/polypyrrole nanoveneer with a Au layer was peeled off from the silicon wafer by Scotch tape. The 80 nm Au film was deposited *via* thermal evaporation on the SWNT side of the nanoveneer through a shadow mask to form source and drain electrodes. The channel length was 30 μm. The nanoveneer with well-defined source, drain, and gate electrodes was immersed into an ammonia solution (3 mol/L) for 12 h to change the polypyrrole layer from a conductive state into an insulating state. This insulating polypyrrole layer can act as the dielectric in the SWNT thin film transistor. The $I-V$ measurements were carried out on a probe station using a Keithley 4200 semiconductor characterization system in the FET configuration. The typical results for the random SWNT thin film transistor are shown in Figure S6.

Acknowledgment. This work was supported by the National Natural Science Foundation of China (Grants 20973013, 51072004, 50821061) and The Ministry of Science and Technology of China (Grants 2007CB936203, 2011CB933003, 2011CB921903).

Supporting Information Available: Additional figures of nanoveneer characterization and the SWNT/polypyrrole thin film transistor. This material is available free of charge *via* the Internet at http://pubs.acs.org.

REFERENCES AND NOTES

1. Blom, P. W. M.; Mihailetchi, V. D.; Koster, L. J. A.; Markov, D. E. Device Physics of Polymer: Fullerene Bulk Heterojunction Solar Cells. *Adv. Mater.* **2007,** *19*, 1551–1566.
2. Bhattacharya, P.; Ghosh, S.; Stiff-Roberts, A. D. Quantum Dot Opto-Electronic Devices. *Annu. Rev. Mater. Res.* **2004,** *34*, 1–40.
3. Medalsy, I.; Klein, M.; Heyman, A.; Shoseyov, O.; Remacle, F.; Levine, R. D.; Porath, D. Logic Implementations Using a Single Nanoparticle−Protein Hybrid. *Nat. Nanotechnol.* **2010,** *5*, 451–457.
4. Avouris, P.; Chen, Z. H.; Perebeinos, V. Carbon-Based Electronics. *Nat. Nanotechnol.* **2007,** *2*, 605–615.
5. Li, Y.; Qian, F.; Xiang, J.; Lieber, C. M. Nanowire Electronic and Optoelectronic Devices. *Mater. Today* **2006,** *9*, 18–27.
6. Geim, A. K.; Novoselov, K. S. The Rise of Graphene. *Nat. Mater.* **2007,** *6*, 183–191.
7. Zhang, T.; Nix, M. B.; Yoo, B. Y.; Deshusses, M. A.; Myung, N. V. Electrochemically Functionalized Single-Walled Carbon Nanotube Gas Sensor. *Electroanalysis* **2006,** *18*, 1153–1158.
8. Gao, M.; Dai, L.; Wallace, G. G. Biosensors Based on Aligned Carbon Nanotubes Coated with Inherently Conducting Polymers. *Electroanalysis* **2003,** *15*, 1089–1094.
9. Ferrer-Anglada, N.; Kaempgen, M.; Roth, S. Transparent and Flexible Carbon Nanotube/Polypyrrole and Carbon Nanotube/Polyaniline pH Sensors. *Phys. Status Solidi B* **2006,** *243*, 3519–3523.
10. Hsieh, C. H.; Cheng, Y. J.; Li, P. J.; Chen, C. H.; Dubosc, M.; Liang, R. M.; Hsu, C. S. Highly Efficient and Stable Inverted Polymer Solar Cells Integrated with a Cross-Linked Fullerene Material as an Interlayer. *J. Am. Chem. Soc.* **2010,** *132*, 4887–4893.
11. Bhattacharyya, S.; Kymakis, E.; Amaratunga, G. A. J. Photovoltaic Properties of Dye Functionalized Single-Wall Carbon

Nanotube/Conjugated Polymer Devices. *Chem. Mater.* **2004,** *16*, 4819–4823.
12. Landi, B. J.; Raffaelle, R. P.; Castro, S. L.; Bailey, S. G. Single-wall Carbon Nanotube–Polymer Solar Cells. *Prog. Photovolt: Res. Appl.* **2005,** *13*, 165–172.
13. Hou, Y.; Cheng, Y.; Hobson, T.; Liu, J. Design and Synthesis of Hierarchical MnO_2 Nanospheres/Carbon Nanotubes/Conducting Polymer Ternary Composite for High Performance Electrochemical Electrodes. *Nano Lett.* **2010,** *10*, 2727–2733.
14. Chen, J.; Liu, Y.; Minett, A. I.; Lynam, C.; Wang, J.; Wallace, G. G. Flexible, Aligned Carbon Nanotube/Conducting Polymer Electrodes for a Lithium-Ion Battery. *Chem. Mater.* **2007,** *19*, 3595–3597.
15. Wu, Q.; Xu, Y.; Yao, Z.; Liu, A.; Shi, G. Supercapacitors Based on Flexible Graphene/Polyaniline Nanofiber Composite Films. *ACS Nano* **2010,** *4*, 1963–1970.
16. Spinks, G. M.; Mottaghitalab, V.; Bahrami-Samani, M.; Whitten, P. G.; Wallace, G. G. Carbon-Nanotube-Reinforced Polyaniline Fibers for High-Strength Artificial Muscles. *Adv. Mater.* **2006,** *18*, 637–640.
17. Sreekumar, T. V.; Liu, T.; Min, B.; Guo, H.; Kumar, S.; Hauge, R. H.; Smalley, R. E. Polyacrylonitrile Single-Walled Carbon Nanotube Composite Fibers. *Adv. Mater.* **2004,** *16*, 58–61.
18. Landi, B. J.; Raffaelle, R. P.; Heben, M. J.; Alleman, J. L.; VanDerveer, W.; Gennett, T. Single Wall Carbon Nanotube-Nafion Composite Actuators. *Nano Lett.* **2002,** *2*, 1329–1332.
19. Zhang, X. T.; Song, W. H.; Harris, P. J. F.; Mitchell, G. R.; Bui, T. T. T.; Drake, A. F. Chiral Polymer–Carbon-Nanotube Composite Nanofibers. *Adv. Mater.* **2007,** *19*, 1079–1083.
20. Chen, G. Z.; Shaffer, M. S. P.; Coleby, D.; Dixon, G.; Zhou, W.; Fray, D. J.; Windle, A. H. Carbon Nanotube and Polypyrrole Composites: Coating and Doping. *Adv. Mater.* **2000,** *12*, 522–526.
21. Zhang, X. T.; Zhang, J.; Liu, Z. F. Conducting Polymer/Carbon Nanotube Composite Films Made by *in situ* Electropolymerization Using an Ionic Surfactant as the Supporting Electrolyte. *Carbon* **2005,** *43*, 2186–2191.
22. Peng, H. S. Aligned Carbon Nanotube/Polymer Composite Films with Robust Flexibility, High Transparency, and Excellent Conductivity. *J. Am. Chem. Soc.* **2008,** *130*, 42–43.
23. Wei, C.; Dai, L. M.; Roy, A.; Tolle, T. B. Multifunctional Chemical Vapor Sensors of Aligned Carbon Nanotube and Polymer Composites. *J. Am. Chem. Soc.* **2006,** *128*, 1412–1413.
24. Veedu, V. P.; Cao, A. Y.; Li, X. S.; Ma, K. G.; Soldano, C.; Kar, S.; Ajayan, P. M.; Ghasemi-Nejhad, M. N. Multifunctional Composites Using Reinforced Laminae with Carbon-Nanotube Forests. *Nat. Mater.* **2006,** *5*, 457–462.
25. Jiao, L.; Fan, B.; Xian, X.; Wu, Z.; Zhang, J.; Liu, Z. Creation of Nanostructures with Poly(methyl methacrylate)-Mediated Nanotransfer Printing. *J. Am. Chem. Soc.* **2008,** *130*, 12612–12613.
26. Schmidt, R. H.; Kinloch, I. A.; Burgess, A. N.; Windle, A. H. The Effect of Aggregation on the Electrical Conductivity of Spin-Coated Polymer/Carbon Nanotube Composite Films. *Langmuir* **2007,** *23*, 5707–5712.
27. Chen, X. B.; Devaux, J.; Issi, J. P.; Billaud, D. The Stability of Polypyrrole Electrical Conductivity. *Eur. Polym. J.* **1994,** *30*, 809–811.
28. Kim, B. H.; Kim, M. S.; Park, K. T.; Lee, J. K.; Park, D. H.; Joo, J.; Yu, S. G.; Lee, S. H. Characteristics and Field Emission of Conducting Poly (3,4-ethylenedioxythiophene) Nanowires. *Appl. Phys. Lett.* **2003,** *83*, 539–541.
29. Cui, Y.; Wei, Q.; Park, H.; Lieber, C. M. Nanowire Nanosensors for Highly Sensitive and Selective Detection of Biological and Chemical Species. *Science* **2001,** *293*, 1289–1292.
30. Kong, J.; Franklin, N. R.; Zhou, C. W.; Chapline, M. G.; Peng, S.; Cho, K. J.; Dai, H. J. Nanotube Molecular Wires as Chemical Sensors. *Science* **2000,** *287*, 622–625.
31. Heiduschka, P.; Preschel, M.; Rosch, M.; Gopel, W. Regeneration of an Electropolymerised Polypyrrole Layer for the Amperometric Detection of Ammonia. *Biosens. Bioelectron.* **1997,** *12*, 1227–1231.
32. Cao, Q.; Hur, S. H.; Zhu, Z. T.; Sun, Y. G.; Wang, C. J.; Meitl, M. A.; Shim, M.; Rogers, J. A. Highly Bendable, Transparent Thin-Film Transistors That Use Carbon-Nanotube-Based Conductors and Semiconductors with Elastomeric Dielectrics. *Adv. Mater.* **2006,** *18*, 304–309.
33. Zhang, Y.; Zhang, Y.; Xian, X.; Zhang, J.; Liu, Z. Sorting out Semiconducting Single-Walled Carbon Nanotube Arrays by Preferential Destruction of Metallic Tubes Using Xenon-Lamp Irradiation. *J. Phys. Chem. C* **2008,** *112*, 3849–3856.
34. Choi, H. C.; Kundaria, S.; Wang, D.; Javey, A.; Wang, Q.; Rolandi, M.; Dai, H. Efficient Formation of Iron Nanoparticle Catalysts on Silicon Oxide by Hydroxylamine for Carbon Nanotube Synthesis and Electronics. *Nano Lett.* **2003,** *3*, 157–161.
35. Niu, J.; Zhu, T.; Liu, Z. One-Step Seed-Mediated Growth of 30–150 nm Quasispherical Gold Nanoparticles with 2-Mercaptosuccinic Acid as a New Reducing Agent. *Nanotechnology* **2007,** *18*, 325607.